THE JOURNAL OF PHYSICAL CHEMISTRY Letters

Letter

pubs.acs.org/JPCL

Spatial Mapping of Flow-Induced Molecular Alignment in a Noncrystalline Biopolymer Fluid Using Double Quantum Filtered (DQF) ^{23}Na MRI

Galina E. Pavlovskaya* and Thomas Meersmann

Sir Peter Mansfield Magnetic Resonance Centre, School of Medicine, University of Nottingham, Nottingham NG2 7RD, United Kingdom

ABSTRACT: Flow-induced molecular alignment was observed experimentally in a non-liquid-crystalline bioplymeric fluid during developed tubular flow. The fluid was comprised of rigid rods of the polysaccharide xanthan and exhibited shear-thinning behavior. Without a requirement for optical transparency or the need for an added tracer, ^{23}Na magic angle (MA) double quantum filtered (DQF) magnetic resonance imaging (MRI) enabled the mapping of the anisotropic molecular arrangement under flow conditions. A regional net molecular alignment was found in areas of high shear values in the vicinity of the tube wall. Furthermore, the xanthan molecules resumed random orientations after the cessation of flow. The observed flow-induced molecular alignment was correlated with the rheological properties of the fluid. The work demonstrates the ability of ^{23}Na MA DQF magnetic resonance to provide a valuable molecular-mechanical link.

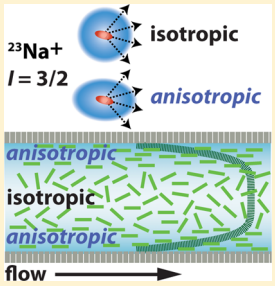

SECTION: Glasses, Colloids, Polymers, and Soft Matter

Rheology of many non-Newtonian fluids is determined by the existence of short-range specific molecular arrangements that define nano- or microstructures of fluids.[1] Molecular arrangements in fluids may be created at different length scales by various interactions between macromolecules, for example, hydrogen bonding, electrostatic interactions, and dispersion interactions, often resulting in the intermolecular chain overlap or chain cross-links in solutions of polymers. Many small molecules are also known to self-assemble into microstructured mesophases of specific length scales, affecting bulk mechanical properties of fluids.[2] Stable microstructures are also known to form in a flow field.[3] These flow-induced structures, widely reported for solutions of wormlike micelles and liquid-crystalline solutions of synthetic polymers and biopolymers, are usually temporary and disintegrate upon flow cessation;[4] however, they alter bulk rheology of fluids, resulting in their shear-banding, shear-thinning, shear-thickening, and nonlinear viscoelastic behavior.[1] Therefore, it is important to characterize these flow-induced structures at the molecular level in order to correlate these structures with macroscopic rheological behavior.

To probe the formation of flow-induced microstructure in fluids, one needs to detect and to characterize short-range molecular order.[1] Contemporary methods that are suited the most for this purpose are small-angle X-ray scattering (SAXS) or small neutron scattering (SANS). Although these methods have been successfully applied to probe short-range molecular order in situ,[4] X-ray transparency of microfluidic devices is required (SAXS methods), or specific fluid manipulation is needed to incorporate tracer particles (SANS methods). Rheo-optical methods necessitate optical transparency of fluids.

Rheo-NMR methods[5] offer a great opportunity to detect molecular order created during deformation of a material within optically opaque media. A small deuterated tracer molecule is usually introduced to the material of interest, and the changes in the quadrupolar coupling constant of deuterium (^{2}H) with shear allow one to deduce the required molecular properties.[6] To date, this approach is probably the most efficient in establishing a molecular-mechanical link in materials studies. Unfortunately, because of the necessity of ^{2}H label incorporation at a fairly high concentration, this method is not readily applicable for biorheological applications, including tissue engineering and in vivo studies.

In this Letter, we propose the use of sodium ions naturally occurring in many biofluids, solutions of biopolymers, and micelles to probe for ordered molecular domains that may be created in these fluids during flow. Due to the nuclear electric quadrupole moment of the isotope ^{23}Na (nuclear spin I = 3/2, 100% natural abundance), sodium ions will experience strong nuclear electric quadrupolar interactions at molecular adsorption sites. However, rapid intra- and intermolecular exchange between different sites and the free solution state will lead to time averaging of the associated quadrupolar couplings. In a biopolymeric solution where molecules will usually assume random orientations, the resulting net quadrupolar coupling vanishes. However, in the anisotropic environment within oriented structural domains, ^{23}Na$^+$ will experience a non-vanishing net nuclear electric quadrupolar coupling. Although the presence of such coupling can readily be seen in single quantum (SQ) ^{23}Na NMR spectra of the liquid-crystalline phase,[7] the weak quadrupolar couplings in flow-aligned molecular domains of biomolecular noncrystalline solutions

Received: May 28, 2014
Accepted: July 16, 2014
Published: July 16, 2014

   dx.doi.org/10.1021/jz501075j | J. Phys. Chem. Lett. 2014, 5, 2632−2636

are masked by heterogeneous line broadening. However, magic angle (MA) double quantum filtered (DQF) ^{23}Na NMR spectroscopy, developed by Navon and co-workers, can be employed for the detection of the unresolved couplings.[8] The method has been shown previously to detect ^{23}Na signal from ordered domains in mostly solid-like structures such as cartilages,[9] pressed blood cells,[10,11] animal cells,[12] and gels formed by polysaccharides.[13] The underlying concept is based on the indirect detection of the second-rank, first-order coherence term $T_{2,\pm1}$. Unlike the $T_{3,\pm1}$ term (third-rank, first-order) that can be generated through multiexponential relaxation in the isotropic phase, as discovered by Bodenhausen and co-workers,[14] the $T_{2,\pm1}$ term is a clear indicator for the presence of coherent evolution. Coherent evolution requires a quadrupolar coupling that is not time-averaged to zero, and the $T_{2,\pm1}$ term is therefore indicative of an anisotropic environment experienced by the sodium ions. The coherence pathway and the detection scheme are described in Figure 1a and b, respectively.

^{23}Na MA DQF spectroscopy and MRI were applied to characterize and image the orientational molecular microstructure created in a flowing model biopolymer solution that does not have an explicit liquid-crystalline phase. This particular model system underlines the potentially higher impact of this technique as many biologically relevant fluids (for example, synovial fluid, blood, and polysaccharide solutions that are used in drug delivery) contain naturally present Na^+ cations and do not have an explicit liquid-crystalline phase but still manifest flow-dependent viscosity in a shear field.[16] Therefore, their mechanical properties are most likely to be governed by hidden microstructural arrangements[17] present at rest and induced by flow. The nature and character of these microstructures are determined by macromolecules and particles that comprise biofluids.

For example, solutions of microbal polysaccharide xanthan exhibit viscoelastic properties in a wide range of concentrations of the dissolved biopolymer[18] in the absence of the liquid-crystalline phase. The structure of the xanthan repeating unit is displayed in Figure 2. Xanthan consists of a cellulose backbone

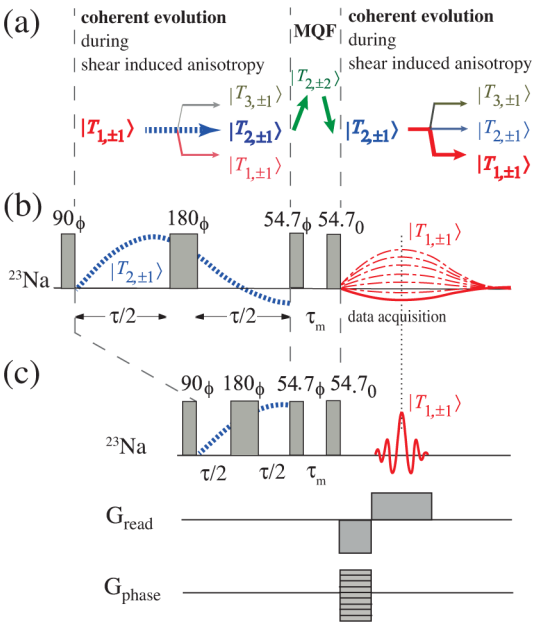

Figure 1. (a) Coherence pathway and (b) MA DQF pulse sequence. ^{23}Na NMR excitation creates coherence described by the tensor element $T_{1,\pm1}$ (i.e., in-phase, SQ coherence). In the presence of a net quadrupolar coupling, the coherence will evolve into higher-rank terms during the two time periods $\tau/2$. Using the appropriate 36-step phase cycling,[9,15] two 54.7° pulses will, via the double quantum (DQ) term $T_{2,\pm2}$, enable only for $T_{2,\pm1}$ coherence to pass the DQ filter. This second-rank (antiphase) coherence term is by itself not directly observable, but it evolves under the net quadrupolar coupling back into detectable $T_{1,\pm1}$ coherence. The presence of a detectable signal after MA DQF provides therefore evidence for coherent quadrupolar evolution that originates from oriented structural domains in the solution. (c) ^{23}Na MA DQF MRI sequence using standard phase and frequency encoding gradients. An echo time $\tau/2 = \tau_{max}/2$ is used to produce maximum $T_{2,\pm1}$ buildup. The gradient echo (GE) is also timed to coincide with maximum $T_{2,\pm1}$ buildup.

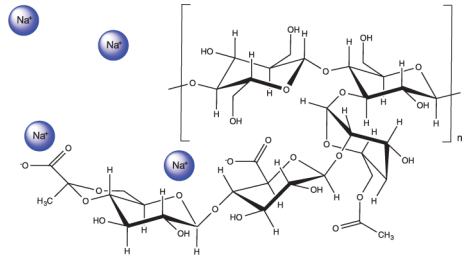

Figure 2. Repeat unit of the polyelectrolyte molecule of xanthan. Na^+ cations interact with the polysaccharide molecule but are also in rapid exchange with free Na^+ in the solution and will exchange intra- and intermolecularly with other repeat units.

with a cellobiose as the repeating unit.[16] Xanthan molecules undergo disorder−order conformational change depending on the salt concentration in the solution.[19] At a 0.5% (w/w) biopolymer concentration and an excess of salt (0.1 M phosphate buffer, pH = 7.0), as also used in the current work, the xanthan molecules will adapt a rigid rod conformation.[18] The fluid appears to be structured in the absence or presence of small deformations, as confirmed by the results of dynamical mechanical analysis (DMA) displayed in Figure 3a. The solid-like structure is already detected at this low biopolymer concentration and persists up to strain values below $\gamma_c = 2.54$. When fluid deformation reaches $\%\gamma_c > 200$, the viscous behavior dominates. With increased shear rate, the fluid exhibits shear-thinning behavior, as shown in Figure 3b. The alignment of polymer rods in a flow field is a plausible explanation for the effect of shear-thinning.[1]

Although bulk rheological data point to the existence of a solid-like structure in the absence of shear (as shown in Figure 3a), this "static structure" is transformed when fluid flows. In principle, new structural domains with net orientation are formed as fluid molecules try to adapt to a flow field, as shown in Figure 4. SQ sodium spectra produced from a static and flowing fluid are very similar, though they originate from different structures formed in this fluid at the molecular level. Hence, the transformation from rest to flow is undetectable from SQ acquisition. In the presence of MA DQF pulses, these structural differences are highlighted, as is evident from the ^{23}Na MA DQF spectra displayed in Figure 4. The static structure produces no net order of molecular orientation, resulting in the absence of a ^{23}Na MA DQF signal, while the flowing sample shows a strong and distinctive ^{23}Na MA DQF signal originating only from the ordered domains created in this fluid by flow.

dx.doi.org/10.1021/jz501075j | J. Phys. Chem. Lett. 2014, 5, 2632−2636

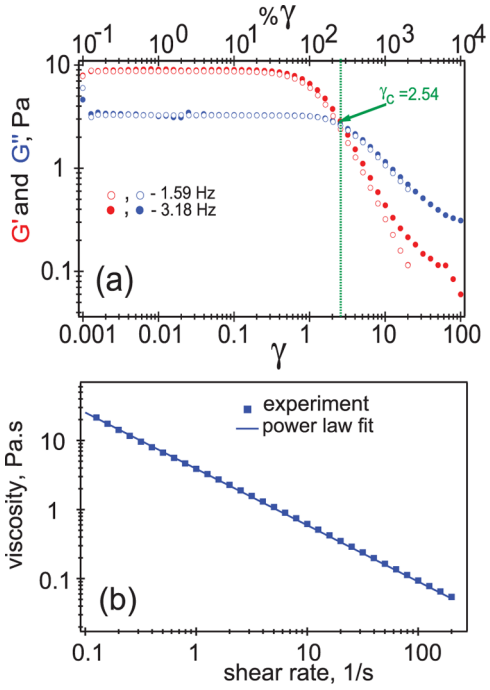

Figure 3. Rheology of 0.5% xanthan in a 0.1 M phosphate buffer, pH = 7.0: (a) Storage G' (red) and loss G'' (blue) moduli at different strains. At lower deformations, elastic behavior dominates up to strain γ_c = 2.54. At deformations above 200%, viscous behavior becomes dominant. (b) Viscosity of the fluid at different shear rates. The fluid exhibits characteristic shear-thinning behavior with viscosity rapidly decreasing with the applied shear rate. Power law model analysis predicts a flow consistency index of K = 3.89 Pa·s and the flow behavior index n = 0.19.

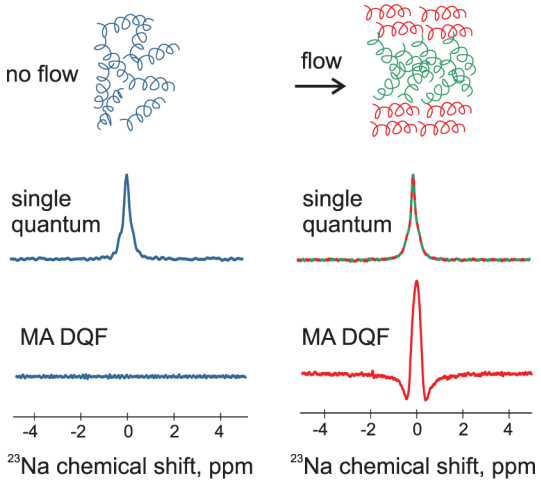

Figure 4. Cartoon of transformation of the xanthan solution structure upon the commencement of flow with alignment created close to the tube wall.[1] The SQ spectrum is the same for the static (blue) and the flowing (red and green) sample. The small quadrupolar coupling from the aligned phase is masked by the line broadening of the resulting SQ spectra. However, the presence of a net quadrupolar coupling during flow is demonstrated by the MA DQF NMR spectrum. No ^{23}Na MA DQF signal is observed in the absence of flow.

The ^{23}Na MA DQF signal evolution as a function of the echo time τ at different flow rates is displayed in Figure 5a. A strong ^{23}Na MA DQF signal $s(\tau,\omega_Q)$ was observed for all the three *Re* numbers studied. The time dependence of the ^{23}Na MA DQF

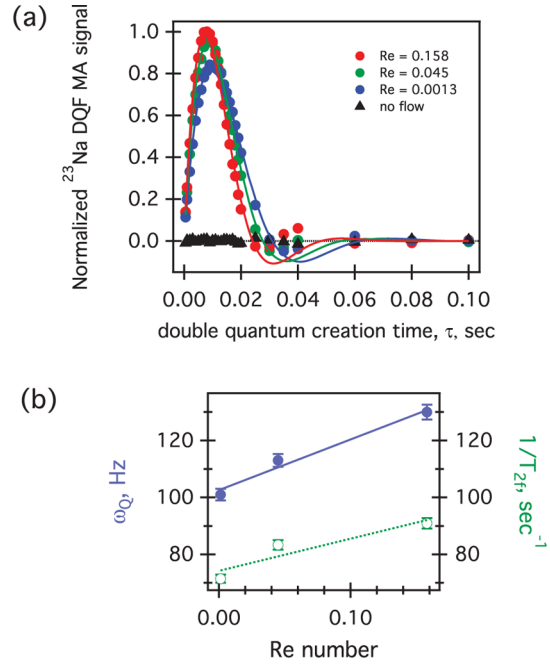

Figure 5. (a) Echo time τ dependence of the ^{23}Na MA DQF signal intensity of a 0.5% xanthan fluid for different *Re* numbers at 9.4 T. The internal diameter of the tube was 19 mm. Experimental data points (filled circles and triangles) reflect the height of the ^{23}Na MA DQF signal after Fourier transformation. Note the absence of the MA DQF signal (black triangles) in the absence of flow. The τ time dependence of the MA DQF signal enables the extraction of the net quadrupolar coupling experienced by the sodium ions. Data fitting with eq 1 are shown as solid lines. (b) Residual quadrupolar coupling constant ω_Q (closed blue circles) and relaxation rate $1/T_{2f}$ (open green circles), extracted from data fitting in (a), are shown as a function of *Re*.

is characterized by the residual quadrupolar coupling constant, ω_Q and the relaxation rate, $1/T_{2f}$[15]

$$s(\tau, \omega_Q) = -C\frac{3}{2}\sin^2(\theta)\sin(\omega_Q\tau)e^{-\tau/T_{2f}} \quad (1)$$

where C is the scaling constant and θ = 54.7° is the tilt angle (i.e., the MA) used for the third and fourth radio frequency pulses shown in Figure 1b. Larger values of ω_Q are indicative of the increased molecular order created. Figure 5b illustrates that ω_Q increases with rising *Re*, indicating increased molecular alignment at higher shear. Furthermore, the relaxation rate $1/T_{2f}$ accelerated with the growing shear, suggesting a reduced molecular mobility in areas with shear-induced alignment.[20] Biexponential relaxation studies[14] should provide further insights into this dynamics but are beyond the scope of this work.

Although ^{23}Na MA DQF spectroscopy identifies the formation of flow-induced structures, it is important to localize them in a flow field. To visualize the spatial occurrence of flow-induced molecular alignments, ^{23}Na MA DQF was incorporated into a gradient echo (GE) imaging sequence, as shown in Figure 1c. In this work, the $\tau/2$ time associated with the maximum $T_{2,\pm1}$ generation, that is, $\tau_{max}/2$, was identified through ^{23}Na MA DQF spectroscopy (Figure 5a) and used for the MRI sequence. In addition, the length of the frequency encoding gradient was adjusted such as the GE was formed at approximately $\tau_{max}/2$ to generate the MA DQF image with the optimal signal-to-noise ratio (SNR). The resulting ^{23}Na MA DQF image is displayed together with SQ ^{23}Na GE (without

dx.doi.org/10.1021/jz501075j | J. Phys. Chem. Lett. 2014, 5, 2632−2636

MA DQF pulses and GE time optimized for the best SNR) and ^{23}Na velocimetry (a time delay with bipolar gradients for flow encoding is inserted right after the 90° pulse and before, optimized for the best SNR GE) MR images in the left panel of Figure 6. All images were acquired during xanthan fluid flow in a tube at a Reynolds number of Re = 0.158. A uniform distribution of Na^+ ions in the xanthan fluid is observed by the SQ ^{23}Na image. However, the MA DQF ^{23}Na MRI signal arises only from domains with some degree of anisotropy. This "telltale" of molecular alignment occurs toward the walls and is absent in the center during flow. The corresponding ^{23}Na velocity image is also shown. Figure 6i depicts the overlay of the traces extracted from the SQ ^{23}Na image with that from the MA DQF ^{23}Na. In Figure 6ii, the center trace from the ^{23}Na velocity image is shown together with the shear profile evaluated from the fitted velocity profile. High shear rates correlate to large velocity differentials and, in the case of pipe flow, are associated with the low velocities found in the vicinity of the wall, and small shear rates are found at the higher velocities in the center. The *in situ* collected data demonstrate that the most intense MA DQF signal, and therefore the highest degree of alignments of xanthan macromolecules, are found at the wall or in the location of the highest shear. As the shear rate becomes smaller toward the center of the pipe, the MA DQF signal becomes less intense and is no longer detected in the center region. This finding suggests that the MA DQF signal, and therefore the flow-induced alignment, closely follow the shear profile under fluid flow.

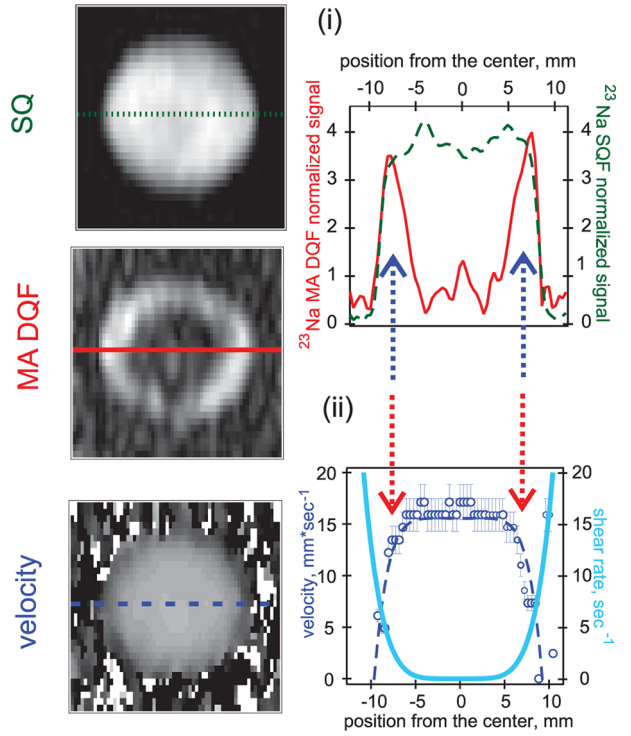

Figure 6. SQ, MA DQF, and velocity ^{23}Na images of xanthan fluid at Re = 0.158. All images were acquired within 1 h using a 9.4 T Bruker Avance III microimaging system at a 105.86 MHz ^{23}Na resonance frequency. The 64 × 16 data matrices were zero-filled and apodized during the data processing. Sixteen gradients were used for flow encoding. (i) SQ (green dashed line) and MA DQF (red solid line) central traces taken along the lines in the corresponding images as shown. (ii) Experimental velocities (blue hollow circles with error bars) and calculated velocity profile (blue dashed line) using the power index n = 0.19 determined from the bulk rheological data in Figure 3b. The shear profile calculated from the velocity profile is shown as a light blue solid line. The regions of high MA DQF signal intensity (i) correlate with the regions of high shear (ii).

For a quantitatively meaningful comparison of the MA DQF data with the observed shear, the effect of various $\tau/2$ times upon the MR images will need to be explored as the $T^2_{\pm1}$ buildup rates might vary across the profile. Nevertheless, in this proof of concept work, the shear profile calculated from the ^{23}Na velocity profile is shown to correlate qualitatively with the areas of alignment obtained from the in situ ^{23}Na MA DQF data. The data correlate well with the previous theoretical finding predicting similar molecular order and suggesting that the molecules will align in the direction of flow.[21]

Unlike bulk rheological data, the molecular-mechanical link provided through ^{23}Na MA DQF allows for noninvasive experimental access to the viscosity heterogeneity in a flowing sample. The technique shows promise for the study of biological fluids and their functionality as the ^{23}Na detection in this work was conducted in the physiological range of sodium concentration. The technique enabled observation of spatially resolved molecular alignment in the absence of an explicit liquid-crystalline phase. Flow-induced structural arrangements might play a significant role in the basic fluid function, and the appearance or absence of flow-induced structures may be used as biomarkers for some diseases, for example, in probing the viability of synovial fluids in joints. The signal intensity is sufficient for MRI applications because ^{23}Na has a 100% natural abundance, possesses a gyromagnetic ratio similar to that of ^{13}C, and undergoes fast quadrupolar relaxation that enables rapid signal averaging.

The technique is easy, straightforward to implement, and noninvasive; therefore, it should also be efficient in providing additional insights into the molecular-mechanical link in systems such as wormlike micelle solutions, liquid-crystalline polymers, colloidal suspensions, hydrogels, and other ^{23}Na-containing soft materials. The molecular-mechanical link is important in many areas of science and technology, including biomedical reseaerch, drug delivery, and tissue engineering.

AUTHOR INFORMATION

Corresponding Author

*E-mail: galina.pavlovskaya@nottingham.ac.uk.

Notes

The authors declare no competing financial interest.

ACKNOWLEDGMENTS

This work was supported by the Medical Research Council under Grant No. G0900785.

REFERENCES

(1) Larson, R. G. *The structure and rheology of complex fluids*; Oxford University Press: New York, 1999.

(2) Cheng, X.; McCoy, J. H.; Israelachvili, J. N.; Cohen, I. Imaging the microscopic structure of shear thinning and thickening colloidal suspensions. *Science* **2011**, *333*, 1276−1279.

(3) Butler, P. Shear induced structures and transformations in complex fluids. *Curr. Opin. Colloid Interface Sci.* **1999**, *4*, 214−221.

(4) Cardiel, J. J.; Dohnalkova, A. C.; Dubash, N.; Zhao, Y.; Cheung, P.; Shen, A. Q. Microstructure and rheology of a flow-induced structures phase in wormlike micellar solutions. *Proc. Natl. Acad. Sci. U.S.A.* **2013**, E1653−E1660.

(5) Callaghan, P. Rheo-NMR: nuclear magnetic resonance and the rheology of complex fluids. *Rep. Prog. Phys.* **1999**, *62*, 599−670.
(6) Lopez-Gonzalez, M.; Holmes, W.; Callaghan, P.; Photinos, P. Shear banding fluctuations and nematic order in wormlike micelles. *Phys. Rev. Lett.* **2004**, *93*, 268302.
(7) Choy, J.; Ling, W.; Jerschow, A. Selective detection of ordered sodium signals via the central transition. *J. Magn. Reson.* **2006**, *180*, 105−109.
(8) Eliav, U.; Shinar, H.; Navon, G. The formation of a 2nd-rank tensor in ^{23}Na double-quantum-filtered NMR as an indicator for order in a biological tissue. *J. Magn. Reson.* **1992**, *98*, 223−229.
(9) Shinar, H.; Navon, G. Multinuclear NMR and microscopic MRI studies of the articular cartilage nanostructure. *NMR Biomed.* **2006**, *19*, 877−893.
(10) Knubovets, T.; Shinar, H.; Navon, G. Quantification of the contribution of extracellular sodium to ^{23}Na multiple-quantum-filtered NMR spectra of suspensions of human red blood cells. *J. Magn. Reson.* **1998**, *131*, 92−96.
(11) Tauskela, J.; Shoubridge, E. Response of the ^{23}Na-NMR double-quantum filtered signal to changes in Na^+ ion concentration in model biological solutions and human erythrocytes. *Biochim. Biophys. Acta* **1993**, *1158*, 155−165.
(12) Fonseca, C.; Fonseca, L.; Montezinho, L.; Alves, P.; Santos, H.; Castro, M.; Geraldes, C. ^{23}Na multiple quantum filtered NMR characterisation of Na^+ binding and dynamics in animal cells: a comparative study and effect of Na^+/Li^+. *Eur. Biophys. J.* **2013**, *42*, 503−519.
(13) Gobet, M.; Mouddab, M.; Cayot, N.; Bonny, J.; Guichard, E.; Le Quere, J.; Moreau, C.; Foucat, L. The effect of salt content on the structure of iota-carrageenan systems: ^{23}Na DQF NMR and rheological studies. *Magn. Reson. Chem.* **2009**, *47*, 307−312.
(14) Jaccard, G.; Wimperis, S.; Bodenhausen, G. Multiple-quantum NMR spectroscopy of S=3/2 spins in isotropic phase — a new probe for mutiexpeonential relaxation. *J. Chem. Phys.* **1986**, *85*, 6282−6293.
(15) Navon, G.; Shinar, H.; Eliav, U.; Seo, Y. Multi-quantum filters and order in tissues. *NMR Biomed.* **2001**, *14*, 112−132.
(16) Dumitriu, S., Ed. *Polysaccharides: structural diversity and functional versatility*, 2nd ed.; Marcel Dekker: New York, 2005.
(17) Picout, D. R.; Ross-Murphy, S. B. Rheology of biopolymer solutions and gels. *Sci. World J.* **2003**, *3*, 105−121.
(18) Rochefort, W.; Middleman, S. Rheology of xanthan gum: salt, temperature, and strain effects in oscillatory and steady shear experiments. *J. Rheol.* **1987**, *31*, 337−369.
(19) Rinaudo, M. Role of substituents on the properties of some polysaccharides. *Biomacromolecules* **2004**, *5*, 1155−1165.
(20) Callaghan, P.; Gil, A. Rheo-NMR of semidilute polyacrylamide in water. *Macromolecules* **2000**, *33*, 4116−4124.
(21) Rapaport, D. C. Shear-induced order and rotation in pipe flow of short-chain molecules. *Europhys. Lett.* **1994**, *26*, 401−406.